Synthetic Biology

DOI: 10.1002/anie.201310645

Reversible Re-programing of Cell–Cell Interactions**

*Kari Gabrielse, Amit Gangar, Nigam Kumar, Jae Chul Lee, Adrian Fegan, Jing Jing Shen, Qing Li, Daniel Vallera, and Carston R. Wagner**

Abstract: *The ability to engineer and re-program the surfaces of cells would provide an enabling synthetic biological method for the design of cell- and tissue-based therapies. A new cell surface-engineering strategy is described that uses lipid-chemically self-assembled nanorings (lipid-CSANs) that can be used for the stable and reversible modification of any cell surface with a molecular reporter or targeting ligand. In the presence of a non-toxic FDA-approved drug, the nanorings were quickly disassembled and the cell–cell interactions reversed. Similar to T-cells genetically engineered to express chimeric antigen receptors (CARS), when activated peripheral blood mononuclear cells (PBMCs) were functionalized with the anti-EpCAM-lipid-CSANs, they were shown to selectively kill antigen-positive cancer cells. Taken together, these results demonstrate that lipid-CSANs have the potential to be a rapid, stable, and general method for the reversible engineering of cell surfaces and cell–cell interactions.*

The ability to coordinate and control cell–cell interactions is a prerequisite for the evolution and development of multicellular life forms. Tissues and organs, such as the central nervous system and immune system, for example, are composed of multiple cellular types. The functioning of these systems is highly dependent on the expression of cell membrane ligands and receptors that direct the interaction between cells. Clearly, the development of approaches for the controlled display of ligands and receptors on cell surfaces would greatly facilitate the ability to manipulate the interactions of cells with other cells and tissues. Furthermore, these methods could also be used to track the behavior of cells in vivo by labeling cells with either optical, radiological, or MRI-detectable probes. A number of approaches have been devised for the re-engineering of cell surface.[1] Bertozzi and Francis have taken advantage of the promiscuity of glycan biosynthesis to randomly terminate cell surface glycoproteins with azidoneuramimic acid, followed by conjugation by click chemistry to oligonucleotides,[2] thus enabling control over cell–cell interactions by differential conjugation to complementary oligonucleotides.[3] Chemical cross-linking methods have also been developed that rely on the random biotinylation of cell surface macromolecules, followed by tethering to a ligand through avidin binding.[4] Although clever, the lack of specificity of these approaches may lead to unforeseen disruptions in either intracellular and extracellular glycoprotein biosynthesis or cell membrane function. Furthermore, while covalent modifications are highly stable, depending on the turnover of the membrane protein or oligosaccharide, they are not reversible.

Non-covalent cell-surface modification approaches have received far less attention. Membrane intercalating proteins or peptides have been conjugated to a phospholipid or fatty acids or linked recombinantly to glycosylphosphatidylinositol (GPI).[5] Chemically reactive fatty acids have been incorporated into liposomes and when allowed to fuse to cell membranes provide chemical conjugation sites to cellular membranes.[6] Although reactive fatty acids have been shown to distribute to the membranes of other cellular organelles, the ability to control cell adhesion to surfaces, including other cells, has been demonstrated.[6] Unfortunately, although membrane protein function may not be directly affected, the association half-life of proteins conjugated to fatty acids or phospholipids is relatively short, ranging from one to two hours.[5,7] Non-cytotoxic polymers have been used to coat cells, while methods have been developed for adhering polyelectrolyte multilayer (PEM) patches to cells using photolithography.[8] While the stability of the association of either polymer or electrolytes to cells is impressive, the modifications are irreversible and, particularly for photolithography, the number of cells that can be modified is limiting. By far the most advanced cell surface modification methods are those that rely on molecular biological techniques to genetically engineer cells to express receptors or ligands. For example, T-cells of adult lymphocytic leukemia (ALL) patients have been engineered to express an anti-CD19 single-chain antibody fused to CD3ε, referred to as chimeric antigen receptors (CARs).[9] The engineered CARs T-cells have demonstrated a remarkable ability to suppress B-lymphocytic tumor growth clinically.[10] Nevertheless, the relatively low transfection efficiency of these methods and the unknown clinical outcome of long lived genetically modified cells are challenges that remain to be addressed.[11] Consequently, a non-genetic approach that would allow the rapid, stable, and reversible modification of membranes with one or more ligands would provide a complementary synthetic biological method for the re-programming of cell surfaces.

[*] K. Gabrielse, A. Gangar, Dr. N. Kumar, Dr. J. C. Lee, Dr. A. Fegan, J. J. Shen, Dr. Q. Li, Dr. C. R. Wagner
Department of Medicinal Chemistry, University of Minnesota
308 Harvard Street SE, Minneapolis, MN 55455 (USA)
E-mail: wagne003@umn.edu
Dr. D. Vallera
Department of Therapeutic Radiology, University of Minnesota (USA)
Dr. C. R. Wagner
Department of Chemistry, University of Minnesota (USA)

[**] We wish to thank Dr. Stephen J. Benkovic and Dr. Dan Harki for their helpful editorial suggestions and the Univ. Minnesota Endowment Fund for financial support.

Supporting information for this article is available on the WWW under http://dx.doi.org/10.1002/anie.201310645.

Our laboratory has developed a method for the engineering and preparation of chemically self-assembled nanorings (CSANs).[12] CSANs are prepared by taking advantage of the power of high affinity chemically induced dimerization.[13] Previously, we had found that when mixed with a covalently linked dimer of the dihydrofolate reductase (DHFR) inhibitor methotrexate (bisMTX), DHFR forms highly robust protein dimers with an affinity of approximately 10^{-11} M.[12] When one DHFR is recombinantly fused through an encoded linker peptide to another DHFR (yielding DHFR-DHFR or $DHFR^2$), we observe spontaneous and rapid self-assembly into CSANs, whose diameter is dependent on the length and composition of the linker peptide (13 amino acid linker = dimer, 1 amino acid linker = octamer).[14] The rings exhibit high stability with T_ms ranging from 63–66 °C (Supporting Information, Figure S7). Single-molecule experiments have also confirmed that even at picomolar concentrations, nearly 70 % of the nanorings remain intact (unpublished data). As the CSANs exhibit the properties of a stable scaffold, we have prepared CSANs recombinantly fused to single-chain antibodies (scFvs) and peptides that target cell-surface receptors.[14,15] The resulting monovalent, bivalent, or octavalent targeted CSANs were found to selectively bind targeted cellular receptors. For example, octavalent anti-CD3 CSANs were shown to bind CD3 + lymphocytic cells with an affinity of 0.9 nM,[14] while CSANs displaying the cyclic-RGD peptide were shown to target $\alpha_v\beta_3$ on breast cancer cells and deliver antisense DNA.[15]

Recently, we have expanded the utility of CSANs by designing and preparing new bis(MTX) chemical dimerizers that contain a third arm with a reactive group capable of being conjugated to fluorophores, drugs, and oligonucleotides.[15,16] Furthermore, we have demonstrated that CSANs can undergo rapid disassembly, both extra- and intracellularly, in the presence of clinically relevant doses of the non-toxic FDA approved bacterial DHFR inhibitor, trimethoprim; thus affording pharmacological and therefore temporal control of their interactions with cells and tissues.[14,16a]

Given our experience with targeted CSANs, we hypothesized that 1) stable membrane intercalating lipid-CSANs might be prepared from $DHFR^2$ and bis-MTX conjugated to a phospholipid; 2) 100 % of the cells would be stably modified when treated with lipid-CSANs; and 3) the lipid-CSANs can be easily removed by exposure to trimethoprim (Scheme 1). If successful, our approach would offer an alternative strategy for the reversible reprogramming of cell surfaces and consequently cell–cell interactions.

We first synthesized a phospholipid-PEG-bis(methotrexate) **3** by preparing bis(MTX) containing a free thiol (**2**) from the protected trifunctional bis(MTX) compound **1** (Scheme 2). Compound **2** was then conjugated to dipalmitoyl phosphatidyl containing a PEG linker and a terminal maleimide in phosphate buffer, pH 7, yielding **3** (Scheme 2; Supporting Information). To insure that the glycocalyx on the cell surface would not hinder binding of the lipid-CSANs, we hypothesized that the combined length of the PEG linker of greater than 30 nM would facilitate cell surface binding of the lipid-CSANs, while the incorporation of dipalmitoyl phosphatidyl choline would enable rapid and stable insertion into cell or liposomal membranes.[17]

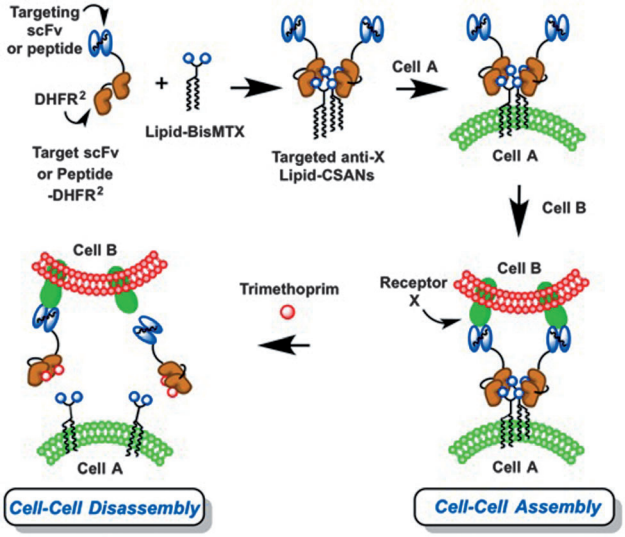

Scheme 1. Cell–cell assembly and disassembly with targeted lipid-CSANs. The representation shows the self-assembling formation of the lipid-CSANs from a recombinant fusion protein of DHFR-DHFR ($DHFR^2$) and a targeting scFv or peptide, followed by spontaneous insertion into the lipid bilayer of a cell membrane (cell A). Incubation with the target cells (cell B) that over-express receptor (X) results in directed cell–cell interactions. In the presence of an excess of trimethoprim, the directed cell–cell interactions undergo rapid disassembly.

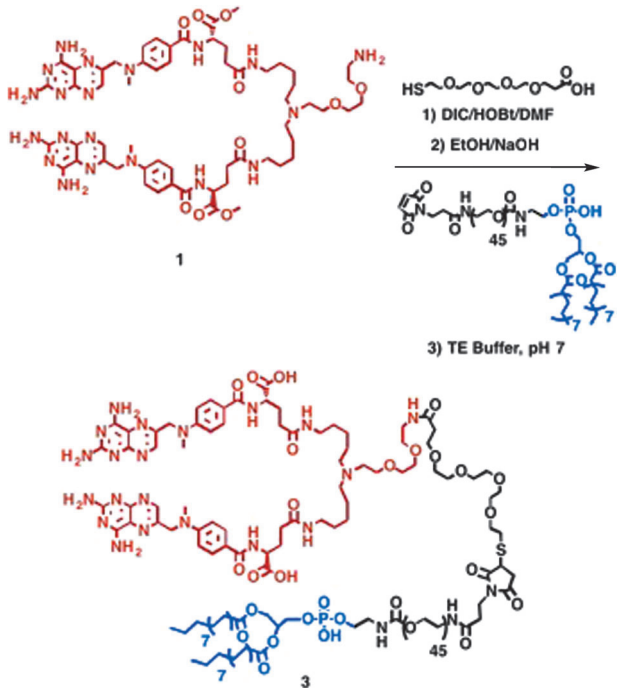

Scheme 2. Synthesis of phospholipid-PEG-bis(methotrexate) (**3**). See the Supporting Information for experimental details.

To test our hypothesis, we first fluorescently labeled $DHFR^2$ proteins containing a thirteen amino acid linker (13-

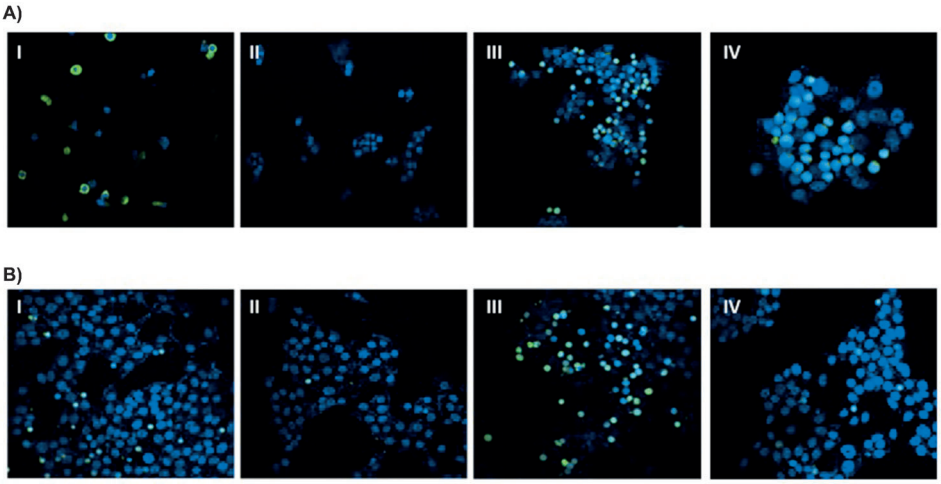

Figure 1. Confocal images of lipid-CSAN-induced cell–cell association and dissociation. A) HPB-MLT (T-leukemia, cells DAPI stained nucleus (blue)) cells treated with Bodipy (green) labeled bivalent lipid-CSANs (**I**). MCF-7 (EpCAM+, DAPI stained nucleus blue) cells incubated with untreated HPB-MLT (CFSE stained green) (**II**). HPB-MLT cells pretreated with bivalent (**III**) or octavalent (**IV**) anti-EpCAM lipid CSANs, respectively, and MCF-7 cells. B) HPB-MLT cells treated with bivalent (**I** and **II**) or octavalent (**III** and **IV**) anti-EpCAM lipid CSANs and incubated with MCF-7 cells, followed by washing with media (**I** and **III**) or washing followed by treatment with excess trimethoprim (**II** and **IV**). See the Supporting Information for details and Table S1 for cell binding statistics.

$DHFR^2$) at an inserted C-terminal cysteine with the dye, Bodipy. Incubation of each protein with **3**, as observed by size-exclusion chromatography (SEC), resulted in the predicted formation of the corresponding bivalent lipid-CSANs (Supporting Information, Figure S2). The T-leukemia cell line, HPB-MLT, was then treated directly with the fluorescently labeled lipid CSANs. As can be seen from Figure 1 A:I, the cell membranes were rapidly and uniformly labeled. When the concentration is lowered, the lipid CSANs were found to associate with distinct regions of the cell membrane that coincide with lipid raft staining (Supporting Information, Figure S3). When labeled cells were washed hourly, no loss of the lipid CSANs was observed over the course of three and half hours (Supporting Information, Figure S4). Over the course of 24, 48, and 72 h, confocal microscopy analysis revealed little or no loss of the lipid CSANs from the cell membrane following washing of the cells every 24 h (Supporting Information, Figure S5).

When quantitated by flow cytometry analysis by measuring the mean fluoresence, an 8% loss of the lipid CSANs was observed over the first 24 h, followed by 80% loss over the next 24 h (48 h) and no appreciable loss over the final 24 h (72 h) (Supporting Information, Figure S6). As the binding thermodynamics of the lipid-CSANs to the membrane should not vary with time, the effect of dilution due to cellular division is likely to be the reason for the observed lower concentration of the observed lipid-CSANs on the cell surface over this time period, as well at the heterogeneity of lipid raft formation.

To investigate the ability of lipid-CSANs to not only modify the cell surface but also direct cell–cell interactions, we chose to prepare lipid-CSANs capable of targeting the cancer antigen epithelial cell adhesion molecules (EpCAM). Epithelial cell adhesion molecules (EpCAM) are single transmembrane glycoproteins that are involved in the regulation of cell–cell adhesion and are over-expressed on a number of epithelial cancers, including colorectal, pancreatic, liver, ovarian, and breast cancer.[18] Furthermore, cancer stem cells have been shown to express EpCAM. We therefore chose to extend our approach by fusing an anti-EpCAM scFv to both 1-$DHFR^2$ and 13-$DHFR^2$. These proteins were then treated with **3**, thus forming anti-EpCAM bivalent and multivalent lipid-CSANs (anti-EpCAM-lipid-CSANs). The ability of HPB-MLT cells treated with anti-EpCAM-lipid-CSANs to bind to the EpCAM positive breast cancer cell line, MCF-7 was then determined. As can be seen from Figure 1 A:II–IV, after washing, untreated HPB-MLT cells did not adhere to MCF-7 cells. However, based on cell image analysis 50- and 70-fold more HPB-MLT cells treated with either the bivalent and octavalent anti-EpCAM CSANs, respectively, were found bound to MCF-7 cells after washing (Figure 1 I,III; Supporting Information, Table S1). Further analysis revealed that the anti-EpCAM-lipid-CSANs treated HPB-MLT cells tended to be found associated with cell junctions, which are known to be EpCAM-rich.[19]

Previously we have shown that upon the addition of excess trimethoprim, a non-toxic competitive inhibitor of DHFR, CSANs can undergo rapid extracellular and intracellular disassembly.[14,16a] To determine if the HBP-MLT cells treated with anti-EpCAM-lipid-CSANs could be released when bound to MCF-7 cells, we incubated HPB-MLT cells that had been functionalized with anti-EpCAM-lipid-CSANs and bound to MCF-7 cells with a twenty fold excess of trimethoprim for 2 h. As can be seen in Figure 1 B:II, IV, cells bearing both the bivalent and multivalent anti-EpCAM-lipid-CSANs were released from the MCF-7 cells, resulting in a loss of approximately 85% of the HPB-MLT cells over this time period (Supporting Information, Table S1). Following our initial success redirecting anti-EpCAM-lipid-CSAN-modified HPB-MLT cells towards MCF-7 cells, we next applied our method toward directing T-cells to induce target cell apoptosis. Activated PBMCs were first treated with anti-EpCAM-lipid-CSANs (1 μM) for two hours, centrifuged to remove excess anti-EpCAM CSANs, and incubated with MCF-7 cells at various ratios of PBMCs/MCF-7 cells (E/T) for 4 h. The amount of cell lysis was determined by the lactate dehydrogenase (LDH) release assay and compared to non-functionalized PBMCs and PBMCs treated with an irrelevant anti-CD22-lipid-CSANs.[20] After 4 h, a twofold increase in cell

lysis was observed for E/T ratios ranging from 1:1 to 50:1 compared to untreated or irrelevant controls, with 90% cell lysis achieved at an E/T ratio of 50:1 (Figure 2A; Supporting Information, Figure S7). These results compare favorably with the observed induced cell lysis of EpCAM positive tumor cells in vitro for anti-CD3 X anti-EpCAM bispecific antibodies over the same time period.[21] To determine the dependence of the observed T-cell induced cell lysis on the loading concentration of the anti-EpCAM-lipid-CSANs, the amount of cell lysis was determined for variable concentrations of anti-EpCAM-lipid-CSANs at a fixed E/T ratio of 10:1. As can be seen from Figure 2B, for 1.5×10^5 cells, a concentration as low as 50 nM of the anti-EpCAM-lipid-CSANs was able to generate maximum cell lysis.

To observe the selectivity of anti-EpCAM-lipid-CSAN-modified PBMCs, we performed time-lapse microscopy. Our target MCF-7 cells were co-cultured with EpCAM-negative U87 glioblastoma cells at a one to one ratio. Upon the addition of anti-EpCAM CSANs treated PBMCs (at a E/T ratio of 1:2), we observed, over the course of 20 h, specific and selective cell lysis of the MCF-7 cells, while the U87 cells remained healthy and maintained a normal morphology (Figure 2C). While the U87 cells continued to divide and move along the plane of the plate, the anti-EpCAM-lipid-CSAN-modified PBMCs were effectively redirected towards the MCF-7 cells resulting in the initiation of apoptosis between 5 and 15 h (Supporting Information, Movie 1). Cell blebbing, plasma membrane disruption, and in some cases cell rupture were observed (Figure 2C). In contrast, when MCF-7 and U87 cells were incubated with untreated activated PBMCs, no apparent cell lysis was observed (Supporting Information, Movie 2). Consistent with these observations, cytotoxicity studies demonstrated that while the cytotoxicity of the modified PBMCs to MCF-7 cells was significantly

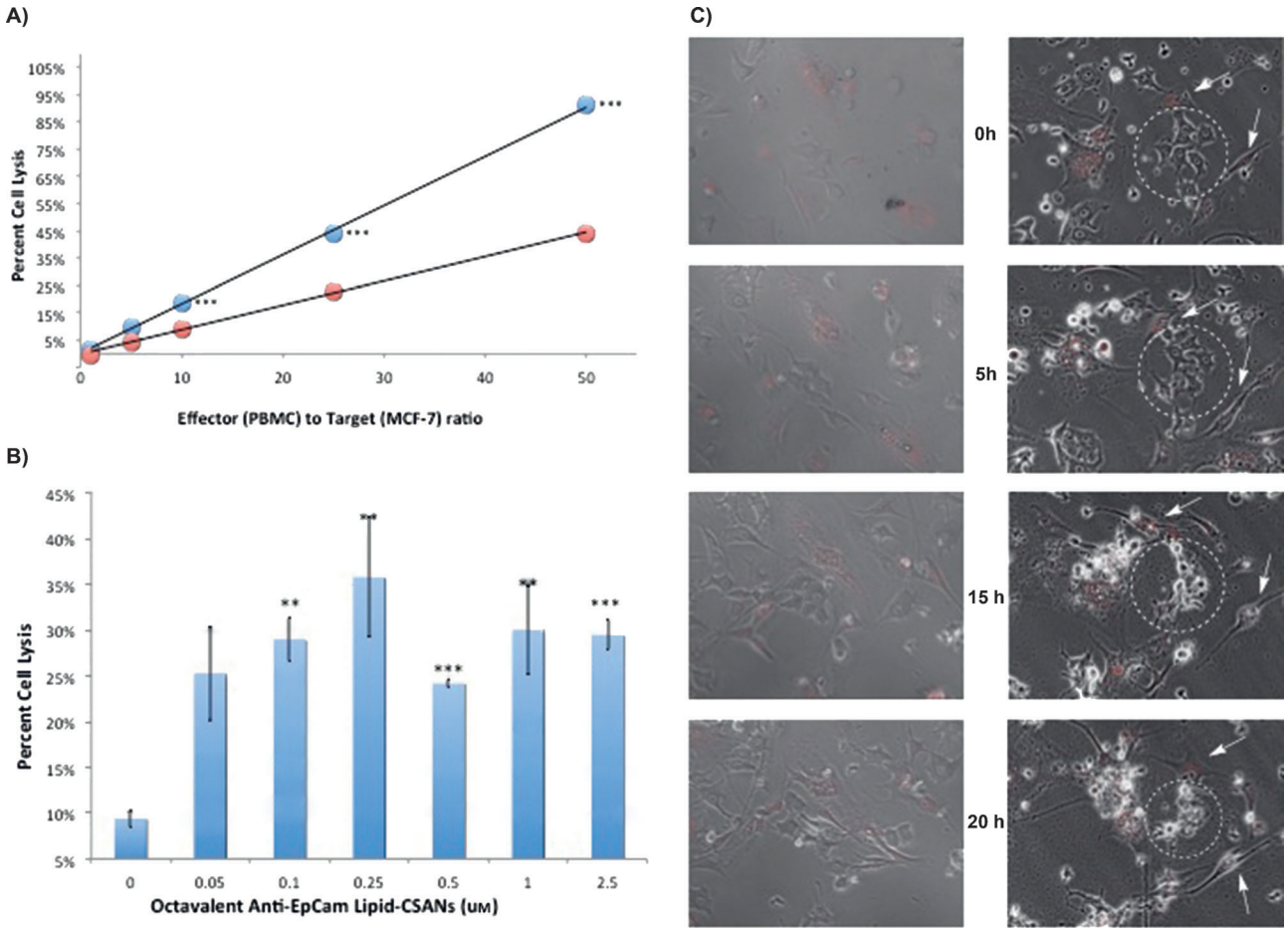

Figure 2. Redirected cell lysis of tumor cells upon incubation with anti-EpCAM lipid-CSAN-modified T-cells. A) Red: Lysis of MCF-7 breast cancer cells over a four-hour incubation time with activated T-cells at varying effector to target (E/T) ratios. Blue: enhanced cell lysis can be observed in the presence of redirected octavalent antiEpCAM lipid-CSAN-treated activated T-cells. *** = $P < 0.0025$. B) Anti-EpCAM lipid-CSAN concentration-dependent cell lysis. Activated PBMCs were treated with varying concentrations of octavalent anti-EpCAM lipid-CSANs, and were then incubated with MCF-7 cells at an E/T ratio of 10:1. *** = $P < 0.003$, ** = $P \leq 0.05$. C) Cell-specific lysis upon incubation with octavalent anti-EpCAM lipid-CSAN-modified T-cells visualized over 20 h (0, 5, 15 and 20 hour time points shown) through time-lapse video microscopy. Cells were cultured at a ratio of two MCF-7 cells to two U87 cells to one PBMC. Left column: a co-culture of MCF-7 breast cancer cells (gray, EpCAM+) and U87 glioblastoma cells (red, EpCAM-) that has been treated with activated T-cells. Right column: octavalent anti-EpCAM lipid-CSANs redirected towards the EpCAM+ MCF-7 cells show an enhanced, cell-specific lysis of MCF-7 cells over EpCAM- U87 cells. White arrows point towards healthy U87 cells, while the white dotted circle encompasses a group of targeted MCF-7 cells. See the Supporting Information for experimental details.

enhanced, no enhanced cytotoxicity to U87 cells was observed (Supporting Information, Figure S6). Thus, the anti-EpCAM-lipid-CSANs are able to not only redirect PBMCs towards the intended target cells, but also to cause selective target antigen directed cell lysis.

Taken together, our results demonstrate that CSANs can be used as a molecular scaffold to stably and non-genetically engineer cell surfaces. Furthermore, temporal pharmacological control over the designed cell–cell interactions can be exerted by treatment with the non-toxic FDA approved antibiotic, trimethoprim. The application of our approach to the design of anti-EpCAM-lipid-CSANs demonstrates that this approach has the potential to be a complementary method for quickly exploring the feasibility of a ligand for adoptive T-cell therapy, as well as a general approach for the development of a synthetic biological method for the reversible modification of cell surfaces and the engineering of cell–cell interactions.

Received: December 8, 2013
Revised: February 17, 2014
Published online: April 2, 2014

Keywords: cell–cell interactions · chimeric antigen receptors · nanoparticles · oligomerization · self-assembly

[1] M. T. Stephan, D. J. Irvine, *Nano Today* **2011**, *6*, 309 – 325.
[2] R. A. Chandra, E. S. Douglas, R. A. Mathies, C. R. Bertozzi, M. B. Francis, *Angew. Chem.* **2006**, *118*, 910 – 915; *Angew. Chem. Int. Ed.* **2006**, *45*, 896 – 901.
[3] J. S. R. D. Rabuka, G. W. deHart, P. Wu, C. R. Bertozzi, *Nat. Protoc.* **2012**, *7*, 1052 – 1066.
[4] H. Cheng, C. J. Kastrup, R. Ramanathan, D. J. Siegwart, M. L. Ma, S. R. Bogatyrev, Q. B. Xu, K. A. Whitehead, R. Langer, D. G. Anderson, *ACS Nano* **2010**, *4*, 625 – 631.
[5] I. K. Ko, T. J. Kean, J. E. Dennis, *Biomaterials* **2009**, *30*, 3702 – 3710.
[6] a) D. Dutta, A. Pulsipher, W. Luo, H. Mak, M. N. Yousaf, *Bioconjugate Chem.* **2011**, *22*, 2423 – 2433; b) D. Dutta, A. Pulsipher, W. Luo, M. N. Yousaf, *J. Am. Chem. Soc.* **2011**, *133*, 8704 – 8713.
[7] J. de Kruif, M. Tijmensen, J. Goldsein, et al., *Nat. Med.* **2000**, *6*, 223 – 227.
[8] a) J. de Kruif, M. Tijmensen, J. Goldsein, T. Logtenberg, *Nano Lett.* **2008**, *8*, 1940 – 1948; b) A. J. Swiston, C. Cheng, S. H. Um, D. J. Irvine, R. E. Cohen, M. F. Rubner, *Nano Lett.* **2008**, *8*, 4446 – 4453.
[9] D. L. Porter, B. L. Levine, M. Kalos, A. Bagg, C. H. June, *N. Engl. J. Med.* **2011**, *365*, 725 – 734.
[10] a) R. J. Brentjens, M. L. Davila, I. Riviere, J. Park, X. Y. Wang, L. G. Cowell, S. Bartido, J. Stefanski, C. Taylor, M. Olszewska, O. Borquez-Ojeda, J. R. Qu, T. Wasielewska, Q. He, et al., *Sci. Transl. Med.* **2013**, *5*, 177ra38; b) D. L. Porter, S. A. Grupp, M. Kalos, A. W. Loren, L. Lledo, J. Gilmore, M. C. Milone, A. Chew, B. L. Levine, C. H. June, *Blood* **2012**, *120*, meeting abstract 717.
[11] K. J. Curran, H. J. Pegram, R. J. Brentjens, *J. Gene Med.* **2012**, *14*, 405 – 415.
[12] J. C. T. Carlson, S. J. Sidhartha, M. Flenniken, T.-F. Chou, R. A. Siegel, C. R. Wagner, *J. Am. Chem. Soc.* **2006**, *128*, 7630 – 7638.
[13] A. Fegan, B. White, J. Carlson, C. R. Wagner, *Chem. Rev.* **2010**, *110*, 3315 – 3336.
[14] a) Q. Li, D. Hapka, H. Chen, D. A. Vallera, C. R. Wagner, *Angew. Chem.* **2008**, *120*, 10333 – 10336; *Angew. Chem. Int. Ed.* **2008**, *47*, 10179 – 10182; b) Q. Li, C. R. So, A. Fegan, V. Cody, M. Sarikaya, D. A. Vallera, C. R. Wagner, *J. Am. Chem. Soc.* **2010**, *132*, 17247 – 17257.
[15] A. Gangar, A. Fegan, S. C. Kumarapperuma, P. Huynh, A. Benyumov, C. R. Wagner, *Mol. Pharmaceutics* **2013**, *10*, 3514 – 3518.
[16] a) A. Fegan, S. C. Kumarapperuma, C. R. Wagner, *Mol. Pharm.* **2012**, *9*, 3218 – 3227; b) A. Gangar, A. Fegan, S. C. Kumarapperuma, C. R. Wagner, *J. Am. Chem. Soc.* **2012**, *134*, 2895 – 2897.
[17] T. Tokunaga, K. Kuwahata, S. Sando, *Chem. Lett.* **2013**, *42*, 127 – 129.
[18] M. Balzar, M. J. Winter, C. J. de Boer, S. V. Litinov, *J. Mol. Med.* **1999**, *77*, 699 – 712.
[19] F. D. Gostner, J. M. Wrullich, O. A. Lehne, F. Zitt, M. Hermann, M. Krobitch, S. Martowicz, A. Gasti, G. Spizzo, *BMC Cancer* **2011**, *11*, 1 – 14.
[20] C. H. Kim, J. Y. Axup, A. Dubrovska, S. A. Kazane, B. A. Hutchins, E. D. Wold, V. V. Smider, P. G. Schultz, *J. Am. Chem. Soc.* **2012**, *134*, 9918 – 9921.
[21] J. Witthauer, B. Schlereth, K. Brischwein, H. Winter, I. Funke, K. W. Jauch, P. Baeuerle, B. Mayer, *Breast Cancer Res. Treat.* **2009**, *117*, 471 – 481.

